BABES-BOLYAI UNIVERSITY CLUJ-NAPOCA

FACULTY OF PHYSICS

Metallic nanostructures with applications in the detection of some bio-molecules

-PhD Thesis-
(summary)

Sorina Garabagiu

Scientific advisor:
Prof. Dr. Simion Aştilean

Cluj-Napoca, 2011

Approved by:

President of the committee: **Prof. Dr. Onuc Cozar**, Dean of the Faculty of Physics, Babes-Bolyai University, Cluj-Napoca

Scientific advisor: **Prof. Dr. Simion Astilean -** Babes-Bolyai University, Cluj-Napoca, Faculty of Physics

Review committee:

Prof. Dr. Dana Dorohoi, Alexandru-Ioan Cuza University, Iasi, Faculty of Physics

CS I. Dr. Ioan Turcu – National Institute for R&D of Isotopic and Molecular Technologies, Cluj-Napoca

Conf. Dr. Dana Maniu, Babes-Bolyai University, Cluj-Napoca, Faculty of Physics

Table of Contents

Motivation and Outline of the Thesis

The aim of this thesis is to develop new detection systems for bio-molecules, by the use of bio-functionalized metallic nanostructures.

The thesis is structured into 3 chapters.

The first chapter presents a review of recent literature in the domain of nanostructures and their bio-sensing applications. It begins with a general presentation of gold nanoparticles, their optical properties, bio-functionalization possibilities and bio-medical applications. Then, a short presentation of anodic aluminium oxide is made, especially as template for nanotubes and nanowires electrodeposition. The chapter ends by presenting the applications of metallic nanowires in biosensors.

The second and third chapters present experimental work and the original contributions of this thesis. In **chapter two**, I detailed two approaches for the fabrication of nanostructures. Gold nanoparticles were obtained by chemical means, while silver nanowires were electrodeposited into anodic aluminium oxide template. A new method for the dissolution of the barrier layer was developed, which offered the possibility to fabricate an array of free-standing silver nanowires, partially embedded into the template.

In **chapter three**, I first demonstrated the bio-functionalization of 25 nm gold nanoparticles using a redox protein: hemoglobin. Then, the results obtained concerning the stability of this complex were used to self-assembly these structures onto a conductive substrate (ITO glass). This gold nanoparticles-hemoglobin modified electrode was used for the electrochemical detection of a neurotoxin found mainly in overcooked food: acrylamide. The detection limit as low as 0,1µM makes this system suitable for the detection of acrylamide levels in food products.

The last few pages of the thesis consist of the main conclusions and original results obtained during the PhD program, and future perspectives.

Keywords: **Metallic nanostructures, Gold nanoparticles, Anodic aluminium oxide, Bio-functionalization, Hemoglobin, Acrylamide, Electrochemical detection**.

Chapter 1: Literature review

1.2.1. Synthesis methods of gold nanoparticles

Among the conventional methods of synthesis of gold nanoparticles (GNP) by reduction of gold(III) derivatives, the most popular one for a long time has been that using citrate reduction of $HAuCl_4$ in water, which was introduced by Turkevich in 1951[1]. The nanoparticles obtained in this way are dispersed in water, having diameters between 10 and 20nm, and have an overall negative surface change due to citrate coverage. The GNP diameter can be controlled by varying the concentration between gold ions and sodium citrate.

Metal nanoparticles of various shapes have been successfully prepared, including nanorods[2], nanoprisms, nano-flowers. Nano-triangles are prepared using aloe-vera leaf extract[3]. Figure 1-1 shows typical TEM images of GNP of different shapes and sizes.

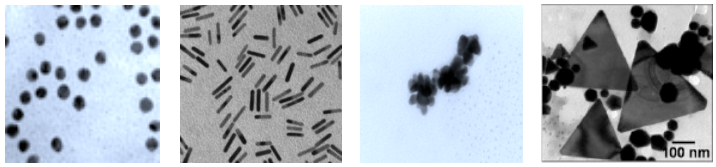

Figure 1-1: TEM images of gold nanoparticles of various shapes and sizes (spheres, nanorods, nano-flowers, nano-triangles)

1.2.2.2. Optical interaction of nanoparticles with fluorescent molecules

Metallic nanoparticles are known to drastically modify the spontaneous emission of nearby fluorescent molecules and materials[4]. Over the past few years, research has focused on determining the form, the extent, the fundamental properties underlying, and the parameters affecting the modification. Especially enhancement of molecular fluorescence has been of great interest due to the widespread popularity of molecular fluorescence based measurements and devices. Applications spanning diverse range of fields such as chemistry, molecular biology, materials science, photonics, and medicine

---

[1] Turkevich J., P. C. Stevenson, J. Hillier - *Discuss. Faraday.Soc*. 11 (**1951**), 55-75
[2] Salata O.V. - *Journal of Nanobiotechnology*, **2004**, 2:3
[3] Prathap S., Chandran, Chaudhary M., Pasricha R., Ahmad A., Sastry M. - *Biotechnol. Prog*., 22(**2006**), 5775583
[4] Tam F., Goodrich G.P., Johnson B.R., Halas N.J.- *Nano.Lett*., 7 (**2007**), 496-501

all rely directly on the inherent brightness of the molecular fluorophore for detection sensitivity.

The fluorescent emission of molecules can be influenced by metallic nanoparticles in several ways:

- By enhancing the optical intensity incident on the molecule via near field enhancement: At the plasmon resonance wavelength of a metallic nanoparticle, the light intensity in the near field of the nanoparticle is enhanced strongly relative to the incident optical wave[5];
- By modifying the radiative decay rate of the molecule[6];
- By increasing the coupling efficiency of the fluorescence emission to the far field through nanoparticle scattering[7].

One of the best defined types of fluorescent signal modification documented in the literature is the quenching of fluorescence by the presence of nanoparticles in the vicinity. In 1999, Templeton and co-workers demonstrated the strong quenching of the emission from the fluorescein moiety by spectrofluorometric measurements when 5-(aminoacetoamido)-fluorescein was bound to tiopronin protected gold nanoparticles[8].Their results indicated a less efficient energy transfer and hence a reduced quenching with increasing linker length. Studies made in our laboratory demonstrated the quenching of porphyrin intrinsic fluorescence in the presence of gold nanoparticles, at an acidic pH[9]. The effect of quenching of fluorescence by gold nanoparticles was studied for some proteins (bovine serum albumin[10]) and dyes (Rhodamine B[11]).

1.2.4. Bio-functionalization of gold nanoparticles

The functionalization of gold nanoparticles with a biomolecular recognition motif have provided flexibility for a variety of applications, including bioassays, bioimaging and biosensing. As a result, the ability to synthesize aqueous stabilized nanoparticles of

---

[5] Dulkeith E., Morteani A.C., Niedereichholz T., Klar T.A., Feldmann J., Levi S.A., van Veggel F.C., Reinhoudt D.N., Möller M., Gittins D.I. - *Phys. Rev. Lett*., 89 (**2002**), 203002
[6] Kitson S.C., Barnes W.L., Sambles J.R.- *Phys. Rev. B: Condens. Matter*, 52 (**1995**), 11441-11445
[7] Szmacinski H., Lakowicz J.R., Johnson M.L.- *Methods Enzymol*., 240 (**1994**), 723-748
[8] Templeton A.C., Cliffel D.E., Murray R.W.- *J.A.C.S*., 121(**1999**), 7081–7089
[9] Mihailescu G., Olenic L, Garabagiu S., Blanita G., Fagadar Cosma E., Biris A.S. - Journal of Nanoscience and Nanotechnology, 10 (**2010**), 2527–2530
[10] Iosin Monica, Canpean V., Astilean S.- *J. Photochemistry and Photobiology A: Chemistry*, 217 (**2011**), 395-401
[11] Zhang H., Wang L. Jiang W. – *Talanta*, 85 (**2011**), 725-729

controlled size and shape that can be easily functionalized with biomolecules (peptides and proteins[12,13], enzymes[14], aminoacids[15], antibodies, DNA) is highly desirable.

It is well established that many functionalities can bind to metallic gold, including sulphur containing moieties such as thiols, thioethers, thioesters, disulfides, isothiocyanates, and then phosphines, amines, citrate, carboxylates, yielding, in all cases, a passivation of the surface that stabilizes nanoparticles preventing their coalescence, although each of these confer a different degree of stability.

1.2.5. Applications of noble metal nanoparticles in bio-detection

The unique properties of noble metal particles have attracted much attention in certain research fields such as medicinal imaging, thermal and/or nonthermal therapy, drug delivery, etc., have also attracted interest in biosensing. The main advantages are the precision, simplicity, and rapidity of such tests.

In addition, they are biological compatible and their surface can be functionalized with a variety of biological molecules[16, 17]. Their reduced size, similar to that of many common biomolecules such as proteins and DNA, facilitates nanoparticles to be integrated into biotechnology.

Nanoparticles with unique optical properties, facile surface chemistry, and appropriate size scale are generating much enthusiasm in molecular biology and medicine. Noble metal, especially Au, nanoparticles have immense potential for cancer diagnosis and therapy on account of their surface plasmon resonance (SPR) enhanced light scattering and absorption. Conjugation of Au nanoparticles to ligands specifically targeted to biomarkers on cancer cells allows molecular-specific imaging and detection of cancer. Additionally, Au nanoparticles efficiently convert the strongly absorbed light into localized heat, which can be exploited for the selective laser photothermal therapy of cancer[18]. By changing the shape or composition of Au nanoparticles, the SPR can be

---

[12] Iosin M., Toderas F., Baldeck P. L., Astilean S. - *Journal of Molecular Structure*, 924-926 (**2009**), 196-200

[13] Tkachenko A.G., Xie H., Coleman D., Glomm W., Ryan J., Anderson M.F., Franzen S., Feldheim **D.L. -** *J.A.C.S.*, 125 (**2003**), 4700-4701

[14] Xiao Y., Patolsky F., Katz E., Hainfeld J.F. ,Willner I. – *Science*, 299 (**2003**), 1877-1881

[15] Selvakannan P.R., Mandal S., Phadtare S., Pasricha R., Sastry M. – *Langmuir*, 19 (**2003**), 3545-3549

[16] Glomm W.R. – *Preparation and characterization of Nanosized Structures with Applications in Bioscience and Materials* (Doctoral Thesis), **2004**

[17] Feldheim D.L., A. Foss Colby Jr. – *Metal Nanoparticles: Synthesis, Characterization, and Applications*, Marcel Dekker, **2002**

[18] Boca S.C., Potara M., Toderas F., Stephan O., Baldeck P.L., Astilean S. - *Mater. Sci.&Eng. C-Materials for Biological Applications*, 31 (**2011**), 184-189

tuned to the near-infrared region, allowing in vivo imaging and photothermal therapy of cancer.

Nanoparticles have been widely used as signal reporters to detect biomolecules in DNA assay, immunoassay and cell bioimaging. Usually, they are derivatized with different functional groups such as nucleic acid-targeted oligonucleotide probes, antibodies and proteins.

The basic principle involved in the design of an optical biosensor based on gold nanoparticles is that the AuNPs are functionalized or capped with a thiolated biomolecule which upon identifying the complementary biomolecule causes change in the optical absorption of AuNPs. For example, aptamer functionalized AuNPs specifically binds to thrombin causing aggregation of AuNPs and red shifting the plasmon peak. Optical biosensors based on nanorods, rather than on nanoparticles are more sensitive to the change of the environmental complex refractive index, due to the existence in the absorption spectrum of a longitudinal plasmon band, in addition to the transversal one, which is not that sensitive to the changes that appeared.

Noble metal nanoparticles adsorb redox enzymes and proteins without losing their biological activity, which makes them suitable in the design of electrochemical biosensors. Gold nanoparticles facilitate electron transfer between the immobilized proteins and bulk electrode surfaces, thus allowing electrochemical sensing to be performed with no need for electron transfer mediators. The most common used nanoparticles-based electrochemical sensors are enzymatic sensors, immunosensors, aptasensors, depending on the active molecule on the surface of the electrode[19]. In the case of enzymatic biosensors, the electric signal is due to an enzymatic reaction, while in the case of immunosensors, the electric signal follows a specific antibody-antigen binding reaction. Aptasensors are based on the DNA base complementarity. Nanoparticles-based electrochemical sensors are mainly used for the detection of various classes of bio-molecules: proteins[20,21], oligonucleotides[22,23], toxins, these sensors being used for raising the quality of life. An important class of biosensors uses the high specificity of the

[19] Guo S., Wang E. - *Analytica Chimica Acta*, 598 (**2007**), 181–192
[20] Zhu S.L., Zhang J.B., Yue L.Y.L., Hartono D., Liu A.Q. - *Advanced Materials Research*, 74 (**2009**), 95-98
[21] Park T.J., Lee S.Y.,Lee S.J., Park J.P., Yang K.S., Lee K.-B.,Ko S., Park J.B., Kim T., Kim S.K., Shin Y.B., Chung B.H., Ku S.-J., Kim D.H., Choi I.S. - *Anal. Chem.* 78 (**2006**), 7197-7205
[22] Elghanian R., Storhoff J.J., Mucic R.C., Letsinger R.L., Mirkin C.A - *Science*, 277 (**1997**), 1078-1081
[23] Baeissa A., Dave N., Smith B.D., Liu J. - *ACS Applied Materials and Interfaces*, 2 (**2010**), 3594-3600

binding between an antibody and its antigen (for instance: biotin-streptavidin[24], albumin-immunoglobulin), which greatly enhance the specificity of the sensor. In this case, the electrochemical signal changes upon the addition of the antibody onto a substrate that already contains the antigen.

A recent application of gold nanoparticles involves their use as carriers for many kinds of drugs, for targeted delivery to a specific organ[25,26].

1.3. Electrochemical synthesis of metallic nanowires

1.3.1.3. Applications of anodic aluminium oxide (AAO)

1.3.1.3.1. AAO template assisted fabrication of nanowires

The self-organized anodization of aluminum, which results in a hexagonal pattern of nanopores with an extended long-range perfect order, appears to be a very promising, powerful and inexpensive method used for the synthesis of nanostructured materials.

Most nanomaterials synthesized with the assistance of anodic porous alumina may be classified into the following groups:

- Metal nanodots, nanowires, nanorods and nanotubes;
- Metal oxide nanodots, nanowires and nanotubes;
- Semiconductor nanodots, nanowires, nanopillars and nanopore arrays;
- Polymer, organic and inorganic nanowires and nanotubes;
- Carbon nanotubes;
- Photonic crystals.

Arrays of metallic nanowires and nanorods are mainly synthesized by the electrodeposition of materials into the nanochannels of anodic porous alumina, or in the AAO template with open pores. Metallic nanowires are deposited into the pores of AAO by chemical or electrochemical means, in the absence, and respectively in the presence of an electric field[27, 28].

---

[24] Hu Y., Song Y., Wang Y., Di, J. **-** *Thin Solid Films*, 519 (**2011**), 6605-6609
[25] Venkatpurwar V.**,** Shiras A.**,** Pokharkar V. **-** *International Journal of Pharmaceutics*, 409 (**2011**), 314-320
[26] Han G., Ghosh P., Rotello V.M. - *Advances in Experimental Medicine and Biology,* 620 (**2007**), 48-56
[27] Martin C.R. –*ACC. Chem. Res*., 28 (**1995**), 61-68
[28] Martin C.R. – *Science*, 266 (**1994**), 1961-1966

Metallic electrodeposition can be realized in both DC (direct current) and AC (alternative current) regimes, and also using current pulses. The main difference between the electrodeposition in DC and AC condition is the necessity to remove the barrier layer formed at the interface between the porous layer and the residual aluminium.

1.3.2. Applications of electrodeposited metallic nanowires

Recently, nanowires and nanorods of metallic and semiconducting materials have drawn a lot of research interest because of their unique physical properties, which are interesting from the view point of different device applications. Nanowires have two quantum-confined dimensions and one unconfined dimension. Therefore, the electrical conduction behavior of nanowires is different from that of their bulk counterpart. In nanowires, electronic conduction takes place both by bulk conduction and through tunneling mechanism. However, due to their high density of electronic state, diameter-dependent band gap, enhanced surface scattering of electrons and phonons, increased excitation binding energy, high surface to volume ratio and large aspect ratio, nanowires of metals and semiconductor exhibit unique electrical, magnetic, optical, thermoelectric and chemical properties compared to their bulk parent counterparts.

The interesting properties of nanowires hold lot of promises for applications in the fields of electronics, optics, magnetic medium, thermo-electronic, sensor devices etc.

Metallic nanowires exhibit interesting plasmon absorption effect. Research has shown that the energy of the surface plasmon band is sensitive to various factors such as particle size, shape, composition, surrounding media and interparticle interactions. It has been reported that changeover from spherical to rod shaped nanostructure leads to splitting from an original single absorption band to two absorption bands that separate and become very prominent with increasing aspect ratio.

The unique properties of nanowires offer excellent prospects for interfacing biological recognition events with electronic signal transduction towards the design of powerful bioelectronic sensors.

Nanowires can be functionalized with different biomolecules, including enzymes, antibodies or nucleic acids, through a variety of established procedures. Such functionalization imparts catalytic and recognition/binding properties onto these 1D nanomaterials. Depending on the specific nanowire material, different functionalization

schemes can be used for confining different biomolecules onto the surface. While molecular linkers (cross-linked to the captured biomolecule) are most commonly used, direct fuctionalization with the biomolecule can also be employed. Template-grown multisegment nanowires can lead to spatially controlled functionalization owing to the distinct surface chemistry of the corresponding segments. The individual segments can thus be modified sequentially with defined spatial control. Such localized functionalization relies on the differential reactivity of the individual segment materials and involves molecular linkages that bind specifically to different segments along the nanowires[29]. The template preparation route facilitates the bio-functionalization of the edges of nanowires, as desired for various (end-to-end) assembly applications.

Enzyme-functionalized nanowires were also designed for on-demand switchable bioelectrocatalytic devices. Magnetic switching (activation) of such bioelectronic devices has been accomplished using bisegment Au/Ni nanowires. Such adaptive nanowires with magnetically activated bioelectrocatalytic processes offer great promise for regulating the operation of biofuel cells, bioreactors, and biosensing devices in response to specific needs. Here, the gold segment serves as the enzyme "carrier" while the nickel one provides the magnetic manipulations. (*Figure 1-5)*[30].

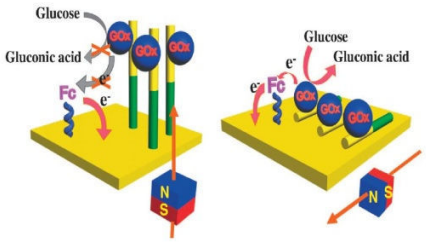

Figure 1-5: Two-component nanowires based biosensor. Magneto-switchable tuning of bioelectrocatalytic processes

Nanowire–biomaterial hybrid systems can offer great potential for different important areas, including multiplexed biosensing, biofuel cells, nanorobotics, nanocircuitry and nanoarchitectures or targeted drug delivery.

[29] Tanase, M., Bauer, L.A., Hultgren, A., Silevitch, D.M., Sun, L., Reich, D.H., Searson, P.C., Meyer, G.J. – *Nano.Lett*., 1 (**2001**), 155-158
[30] Laocharoensuk R., Bulbarello A., Hocevar S.B., Mannino S., Ogorevc B., Wang J. - *J.A.C.S.*, 129 (**2007**), 7774-7775

Chapter 2: Synthesis of noble metal nanostructures

In this chapter I propose the synthesis of gold nanoparticles and the preparation of silver nanowires into the anodic aluminium oxide template.

2.2. Synthesis of gold nanoparticles

Gold nanoparticles were synthesized according to Turkevich method[1]. In this citrate reduction procedure, 100 mL $HAuCl_4$ aqueous solution is heated to its boiling point. Subsequently, sodium citrate is quickly added, resulting in color changes from yellow solution, to transparent, then to dark-blue and finally to burgundy red. The resulting colloidal GNPs are spherical and have an overall negative surface change due to citrate coverage. In this case, aqueous synthesis of GNPs utilizing sodium citrate as both reducing agent and electrostatic stabilizer produced nanoparticles with mean diameter of 25nm (see *Figure 2-3*).

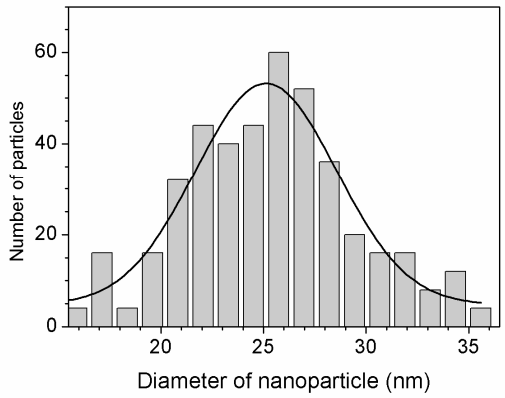

Figure 2-3: Distribution chart of the diameter of gold nanoparticles prepared

2.3. Anodic aluminium oxide fabrication and characteristics

2.3.3. Anodic aluminium oxide characterization

Anodic aluminium oxide (AAO) membranes characterization was performed using microscopic techniques (SEM and AFM). The membranes were prepared in oxalic acid, at 40V, the pores have 40nm in diameter, as shown in the AFM (*Figure 2-6)* and SEM images (*Figure 2-7)* below. The domains of self-ordering of pores have approximately 1 μm^2.

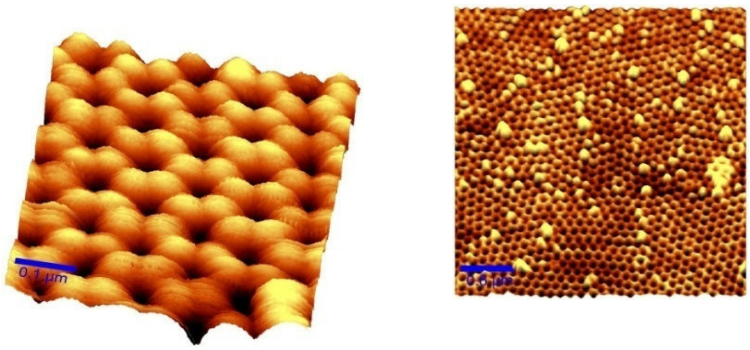

Figure 2-6: AFM images of a porous anodic aluminium oxide membrane, prepared in oxalic acid electrolyte

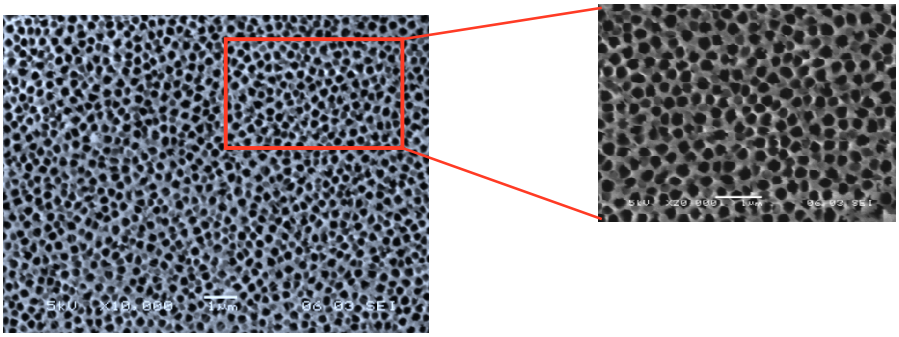

Figure 2-7: SEM images of a porous anodic aluminium oxide membrane, prepared in oxalic acid electrolyte (pores surface)

2.3.4. Electrically controlled dissolution and thinning of the barrier layer

2.3.4.2 Removal of the barrier layer and thinning the membrane

The dissolution of the aluminium oxide barrier layer, formed at the interface between the aluminium base and the porous layer is dissolved using 5% phosphoric acid solution. A new dissolution method was developed in this thesis, with an electrical control of the process. In order to control the dissolution of alumina we used a double electrolytic cell (see *Figure 2-9*). One of the compartments contains phosphoric acid (5%) that dissolves the alumina, and the other contains potassium chloride (1 M), with no effect on the alumina membrane. The AAO membrane was placed between the two compartments, with the barrier layer faced to the acid. The acid dissolves slowly the

membrane, first the barrier layer and then the porous layer. An AC potential was applied between the two platinum electrodes (0.5 or 1 V).

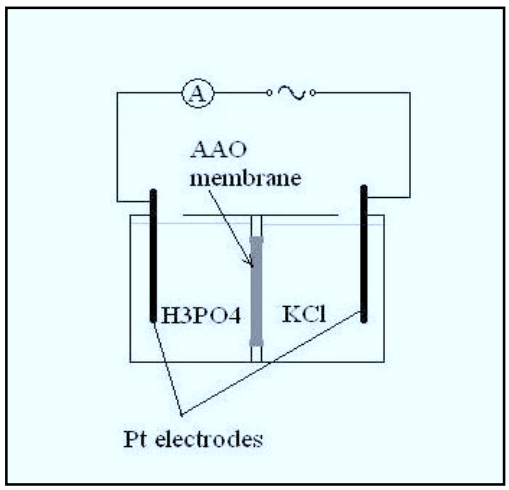

Figure 2-9: Experimental setup for dissolving barrier layer of AAO

The three domains of the plot in *Figure 2-10* correspond as following: the first one is the time that the barrier layer completely removed, then the increasing slope corresponds to opening of pores, and when all pores are opened, the current intensity becomes constant (the third region of the plot) and the membrane is thinning.

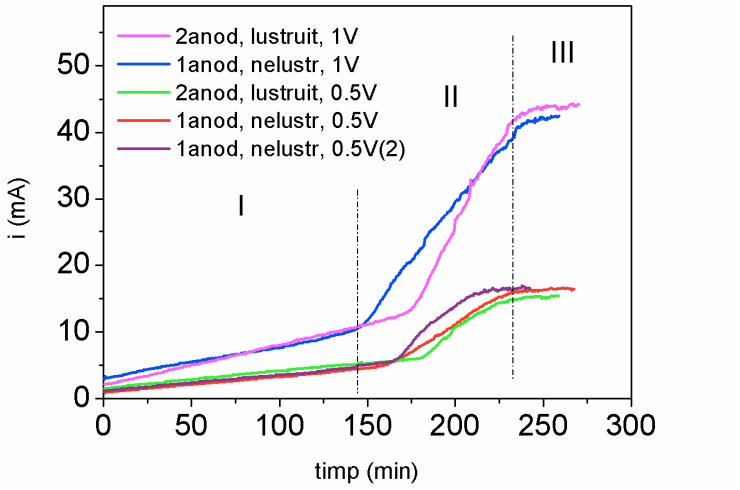

Figure 2-10: Current intensity–time plot of AAO membrane

The dissolution process is not influenced by the potential applied between the two platinum electrodes in the cell, result proved by applying short potential pulses between the electrodes (1-min pulse at every 30 min) (see *Figure 2-12*). Neither the applied potential nor temperature influences the shape of the plot, but increasing the applied potential increases the current intensity and increasing temperature accelerates the process.

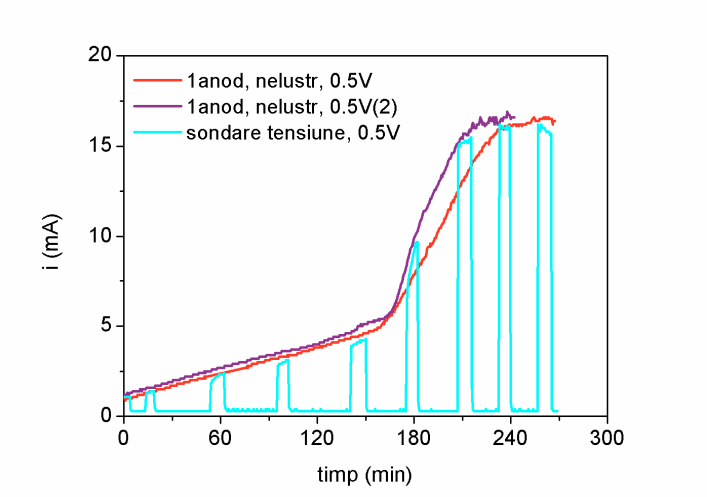

Figure 2-12: Current intensity–time plot of AAO membrane with potential pulses.

This electrically controlled dissolution method is new, being one of the originals contributions of this thesis[31]. This method is further used for the fabrication of a 2D network of silver nanowires.

2.3.5. Study of the optical properties of anodic aluminium oxide films

The alumina membrane is considered to be a thin film, standing freely in air. The film has the thickness d and the complex refractive index n=n−ik, where n is the refractive index and k is the extinction coefficient which can be expressed in terms of the absorption coefficient (α). The refraction index of the surrounding medium is n_0=1.

There is a variation in the thickness of the film, due to anodization parameters (both formation and dissolving of alumina) and to the porous structure of alumina membrane. Inhomogeneities in the film have a large influence on the optical transmission

[31] **Garabagiu S.**, Mihailescu G. – *Materials Letters*, 65 (**2011**), 1648–1650

spectrum. Alumina membranes are regarded as non-uniform thin films with respect to their thickness.

Considering the contribution of barrier layer to the transmission spectrum ($T_{barrier}$) and the porosity of alumina membrane (p), transmission becomes *(2-2):*

$$\mathrm{T} = \mathrm{T_{membrane}}(1 - \mathrm{p}) + \mathrm{T_{pores}}\mathrm{p} + \mathrm{T_{barrier}} \quad (2\text{-}2)$$

where p is the porosity, T_{pores}= transmission through pores.

The refractive index function dependence of the wavelength is given by Cauchy Formula *(2-4):*

$$n = \frac{a}{\lambda^2} + b \quad (2\text{-}4)$$

When the amplitude of oscillations is weak, the accuracy of the calculated values is strongly affected. When there is a great number of extrema in the spectrum, this leads to reduced errors while determining thickness and the order numbers of corresponding extrema.

I studied the refractive index dependence on the wavelength, using both experimental and simulated transmission spectra of anodic aluminium oxide films. From experimental spectra, the values for each maximum and minimum were used, in order to determine a third order function for the corresponding envelopes. Knowing these envelopes, the refraction index is calculated from (*2-6*):

$$n = \left[N + (N^2 - s^2)^{1/2}\right]^{1/2} \quad (2\text{-}6)$$

with $N = 2s\frac{T_M - T_m}{T_M T_m} + \frac{s^2+1}{2}$, and

s = 1 (refractive index of the surrounding medium).

Cauchy interpolation of complex refractive index (see *Figure 2-15*) calculated from the simulations have the coefficients:

a=26140.336,

b=1.556.

Correlation coefficient between experimental and calculated spectrum is r^2=0.97988, which is related to a very good correlation.

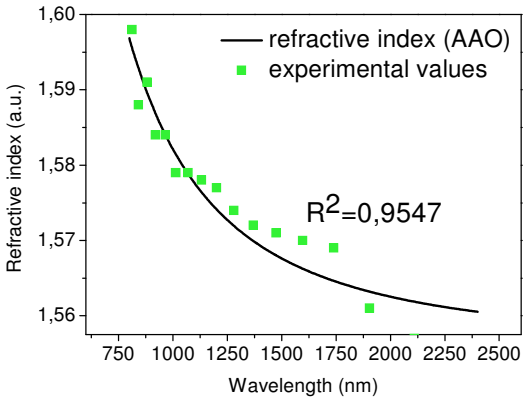

Figure 2-15: Variation of the refractive index with the wavelength

Using the experimental transmission spectra of the film, some parameters were calculated: film thickness=3050 nm (corresponds to the experimental determination: 3±0.1 μm), the variation in the thickness of the film Δd=110±10 nm, barrier layer thickness: 70±25 nm.

Experimental measurements involve modifications of both film thickness and barrier layer thickness, but modification of film thickness has a larger influence on the transmission spectrum, due to a larger contribution of the porous layer to the transmission. Using the experimental setup for dissolving the barrier layer, measuring transmission spectra after several dissolving periods for the same membrane, and calculating the thickness of the films obtained, can be concluded that the dissolution rate of alumina is 0.5±0.1 nm/min, at room temperature (23 °C).

Figure 2-16 shows the good fitting results between the experimental and simulated transmission spectra.

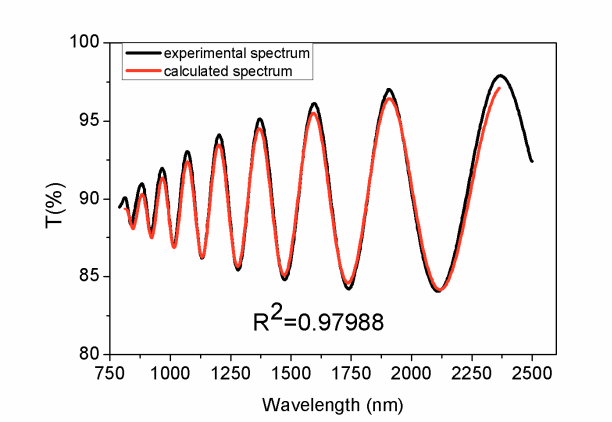

Figure 2-16: Experimental and calculated transmission spectrum of AAO

2.4. Template procedures to prepare metallic nanowires

2.4.4. Fabrication of a silver nanowires array

The main scope was to realize a network of silver nanowires, embedded only partially into the surrounding insulating template[32]. The nanowires were prepared by AC electrodeposition into the AAO pores, and then using the dissolution method presented above, the template surrounding the tips of the wires was dissolved. The membranes used for electrodeposition were obtained in oxalic acid, at 40V and 4°C.

Depending on the dissolution time, the length of the free-standing Ag wires can be controlled. The dissolution plot of barrier layer and then of porous oxide layer surrounding the nanowires is presented in *Figure 2-23*.

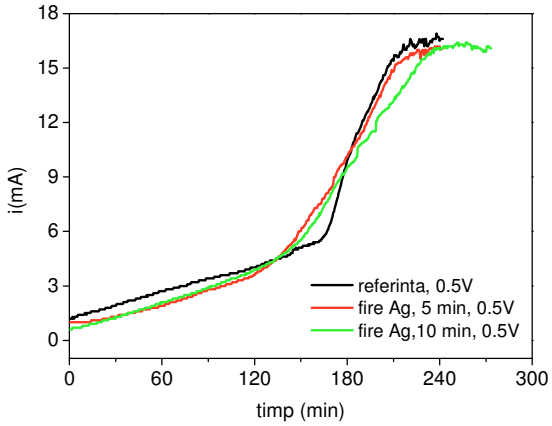

Figure 2-23: Current intensity-time plot of dissolution of barrier layer of AAO, with Ag nanowires embedded, having various deposition times

UV-Vis spectra in *Figure 2-25-A and B* display the nanowires partially embedded into the AAO template, with different ratio between the fraction embedded into the template and the one free-standing in solution. If the dissolution time is longer, some nanowires are detached from the alumina, and therefore the absorption maximum decreases in intensity. The maximum is attributed to the transversal plasmon resonance of silver nanowires. The longitudinal resonances don't appear in the spectrum due to the parallel orientation of nanowires with the incident light. The position of the maximum is shifted due to the changes that appear in the effective refractive index of the dielectric medium (from 401 to 403nm).

[32] Garabagiu S., Mihailescu G., Giloan M. – Template synthesis of metallic nanowires, Journal of Optoelectronics and Advanced Materials, (**2010**) (submitted)

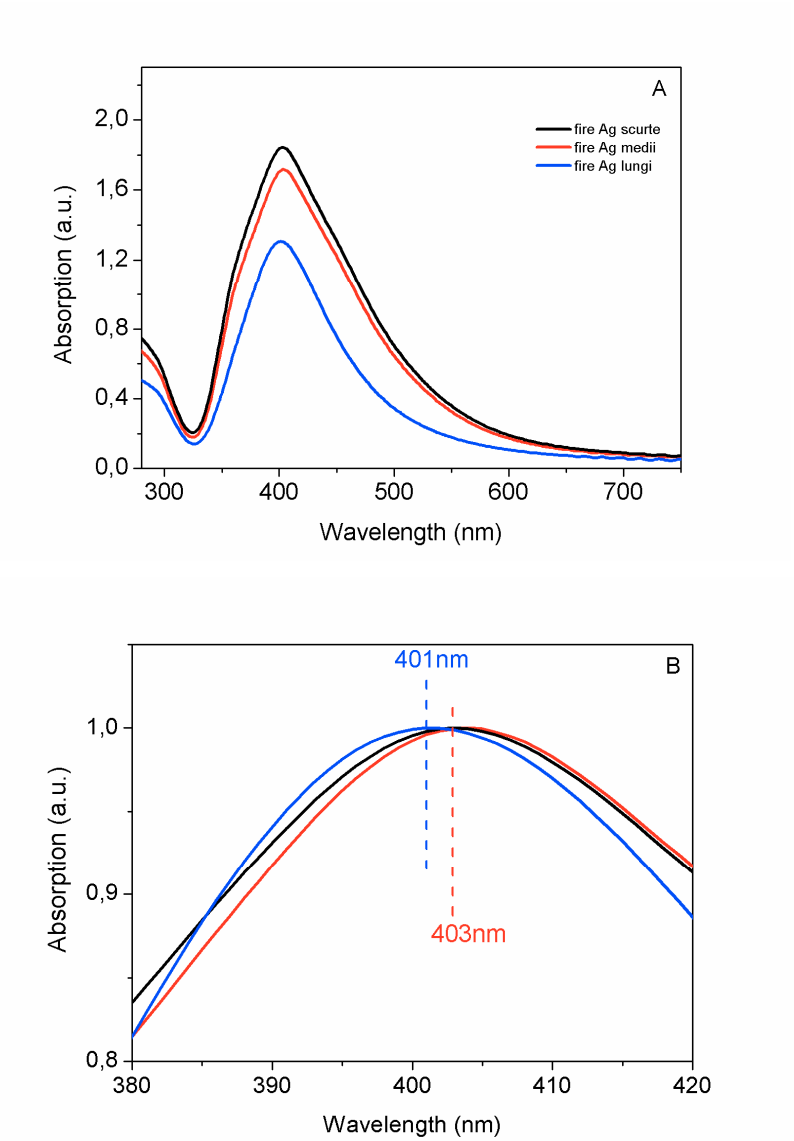

Figure 2-25: A: Absorption spectrum of Ag nanowires after the controlled dissolution processes, for various time intervals; B: Details about the transversal plasmonic shift

Figure 2-26 displays the AFM image of the silver nanowires network obtained, with the tips of the nanowires standing above the alumina template. This array has potential applications as SERS-Surface Enhanced Raman Scattering (or TERS-Tip Enhanced Raman Scattering) substrate, and in biosensors, due to the fact that each nanowire is insulated from each other by the alumina that surrounds it.

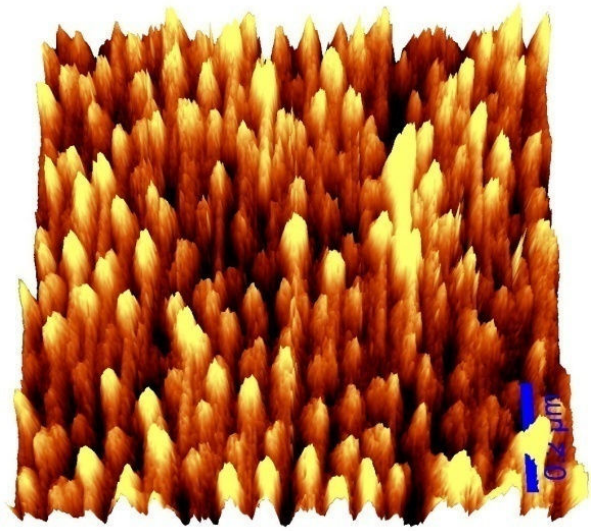

Figure 2-26: AFM image of the Ag nanowires array, partially embedded into the AAO template

Chapter 3: Bio-functionalized gold-nanoparticles based electrochemical detection of a biomolecule

3.2. Hemoglobin

3.2.1. Hemoglobin structure

Hemoglobin (Hb) (*Figure 3-1*) is the red pigment, iron-containing oxygen-transport metallo-protein the red blood cells of all vertebrates. Hemoglobin in the blood carries oxygen from the lungs to the rest of the body, where it releases the oxygen to burn nutrients to provide energy to power the functions of the organism, and collects the resultant carbon dioxide to bring it back to the respiratory organs to be dispensed from the organism. The protein makes up about 97% of the red blood cells' dry content.

Hemoglobin molecule is an assembly of four globular protein subunits. Each subunit is composed of a protein chain tightly associated with a non-protein heme group (*Figure 3-2*). Each protein chain arranges into a set of alpha-helix structural segments connected together in a globin-fold arrangement, so called because this arrangement is the same folding motif used in other heme/globin proteins such as myoglobin.

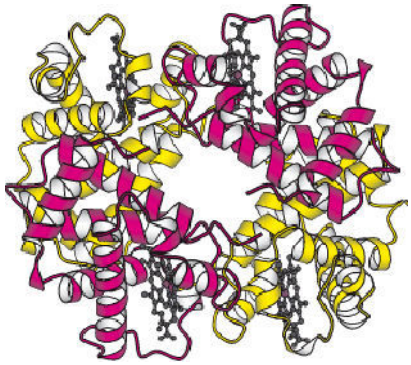

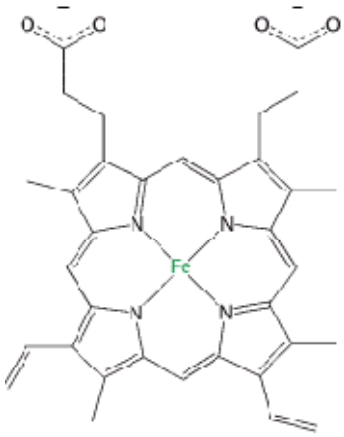

Figure 3-1 (left): Hemoglobin general structure[33]: $\alpha_2\beta_2$ tetramer (heme group in black, the two α units in red and the two β units in yellow)

Figure 3-2 (right): Heme group from the structure of Hemoglobin[33]

3.3. Bio-functionalization of gold nanoparticles using hemoglobin

3.3.1. Formation of the complex gold nanoparticles-hemoglobin

Hemoglobin adsorbs onto gold nanoparticles surface due to the amino and thiolic groups of the aminoacids in its structure. The bio-functionalization of gold nanoparticles using hemoglobin molecules is studied by optical spectroscopy (UV-Vis and Fluorescence Spectroscopy).

3.3.2. UV-Vis Spectroscopy studies

Upon the addition of various concentrations of Hb in the colloidal gold solution, the nanoparticles retained their stability (the solution did not change its color, from red to blue, and the absorption spectra did not change significantly). The red shift (4 nm) that appeared in the UV–Vis spectra of GNP solution upon the addition of various concentrations of Hb (*Figure 3-4*) is due to the changes of the complex refractive index of the surrounding medium of nanoparticles. Hemoglobin concentrations used in this case were: 0 M, $5\text{x}10^{-9}$ M, 10^{-8} M and $2\text{x}10^{-8}$ M.

[33] Berg J.M., Tymoczko J.L., Stryer L - *Biochemistry (Fifth Edition)*, W.H. Freeman and Company, **2002**

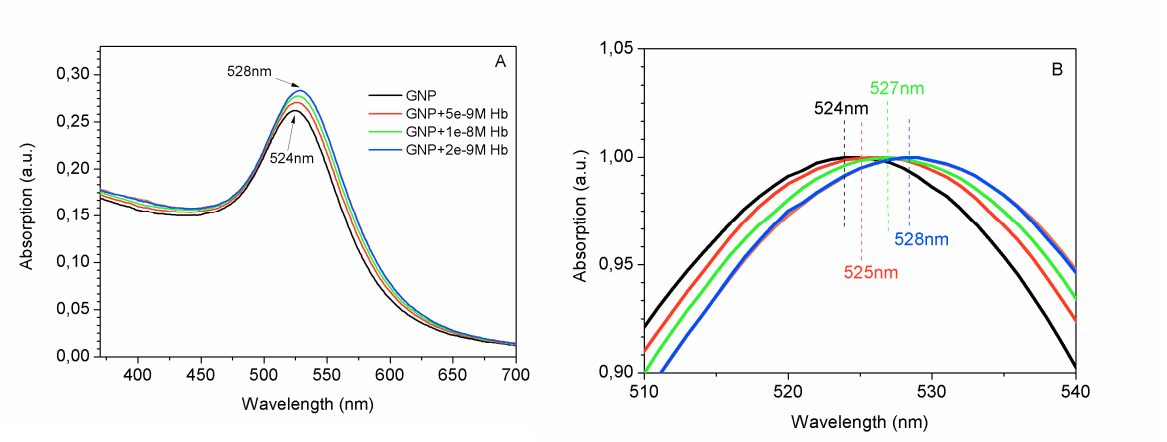

Figure 3-4: A: Absorption spectra of the complex GNP+Hb, upon the addition of various concentrations of Hb; B: The plasmonic resonance shift appeared in the spectrum along with increasing Hb concentration;

If small concentrations of GNP are added to 1 μM Hb solution, the absorption spectra (*Figure 3-6*) reveal the appearance of the absorption enhancement process, at the wavelength corresponding to the plasmon resonance of nanoparticles. Soret band of hemoglobin (406 nm) does not change, meaning that GNP retain the biological function of hemoglobin (upon denaturation, a red shift would appear in the Soret band of Hb). GNP do not interact directly with the heme group out of the Hb structure (at pH = 7.4), as shown in one of our previous studies[9].

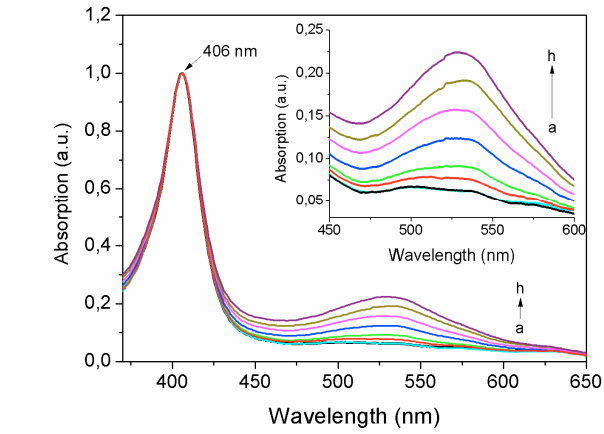

Figure 3-6: UV-Vis spectra of Hb upon the addition of GNP solutions: a) 0M; b) 10^{-12}M; c) $5x10^{-12}$M; d) 10^{-11}M; e) $2x10^{-11}$M; f) $3x10^{-11}$M; g) $4x10^{-11}$M; h) $5x10^{-11}$M

3.3.3. Quenching of intrinsic fluorescence of hemoglobin by gold nanoparticles

The Hb molecule contains three tryptophan residues in each αβ dimer, but only β37-Trp is located at the interface between the two dimers. Intrinsic fluorescence signal of Hb arises from the indole group of this tryptophan residue. This tryptophan plays an important role in the changes that appear in the quaternary structure of Hb upon ligand binding[34, 35].

In this case, GNP quenches the fluorescence of Hb in solution, due to the changes that appear in Hb quaternary structure after the binding. Fluorescence spectra presented in *Figure 3-7* reveals the quenching effect of GNP on the fluorescence emission of tryptophan residues from the protein structure.

As can be seen in *Figure 3-8*, no shift of the fluorescence emission signal appears after the addition of colloidal gold. This indicates that GNP quench the inner fluorescence of Hb molecules and the chemical microenvironment of the fluorescent amino-acid residue in the protein structure do not change appreciable[36].

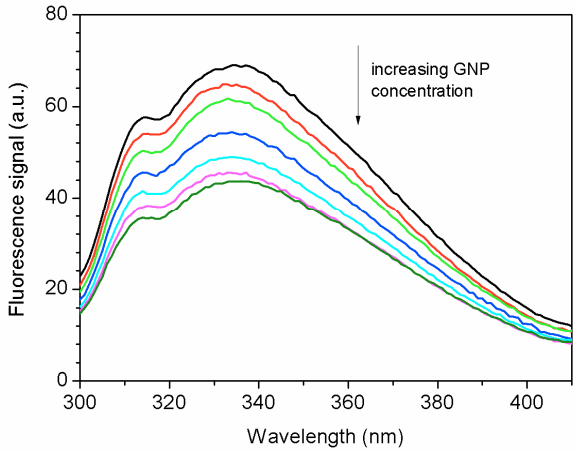

Figure 3-8: Quenching of fluorescence emission of hemoglobin in the presence of various concentrations of GNP (from top to bottom: 0M, 10^{-11}M, $2x10^{-11}$M, $4x10^{-11}$M, $6x10^{-11}$M, $8x10^{-11}$M, 10^{-10}M)

[34] Goldbeck R.A., Esquerra R.M., Kliger D.S. – *J.A.C.S*, 124 (**2002**), 7646-7647
[35] Venkateshrao S, Manoharan P.T. – *Spectrochimica Acta Part A*, 60 (**2004**), 2523-2526
[36] Garabagiu S. - A spectroscopic study on the interaction between gold nanoparticles and hemoglobin, *Mat. Res. Bull.*, (**2011**) (accepted);

The quenching mechanism is described by the Stern–Volmer *equation (3-1):*

$$F_0/F = 1 + K_q\tau_0[GNP] = 1 + K_{SV}[GNP] \quad (3\text{-}1)$$

where:

- F_0 is the fluorescence emission intensity in the absence of the quencher (GNP);
- F is the fluorescence emission intensity in the presence of the quencher;
- K_q is the bimolecular quenching rate constant; τ_0 is the average lifetime of hemoglobin in the absence of a quencher;
- K_{SV} is the Stern–Volmer constant;
- [GNP] is the concentration of the quencher.

Figure 3-9 displays Stern–Volmer plot for the quenching effect of GNP, at two different temperatures: 301 K and 311 K. The Stern–Volmer constants were calculated from experimental data, as listed in *Table 3-1*. The values obtained in this study are much greater than $2x10^{10}$ $l{\cdot}mol^{-1}{\cdot}s^{-1}$, meaning that the quenching was not initiated from dynamic quenching. The Stern–Volmer constant decreases with increasing temperature, meaning that static quenching mechanism is predominant in this case, and a complex Hb-GNP is formed.

For the static quenching interaction, the relationship between the fluorescence intensity and the quenching medium can be deduced using the concentration of bound and unbound Hb molecules in the solution.

The relationship between the fluorescence intensity and the unbound molecules becomes *(3-5):*

$$log\left(\frac{F_0}{F} - 1\right) = \log(K) + nlog[GNP] \quad (3\text{-}5)$$

where:

- K is the binding constant between gold nanoparticles and hemoglobin;
- n= stoichiometry of the complex

From the linearity of the plot in *Figure 3-10*, the value of binding constant and the number of binding sites can be determined, at two temperatures: 301K and 311K. The values are listed in *Table 3-1*. The binding constant increases with increasing the reaction temperature, meaning that at higher temperature, the interaction between Hb and GNP is stronger. A similar conclusion was drawn in the case of silver nanoparticles.

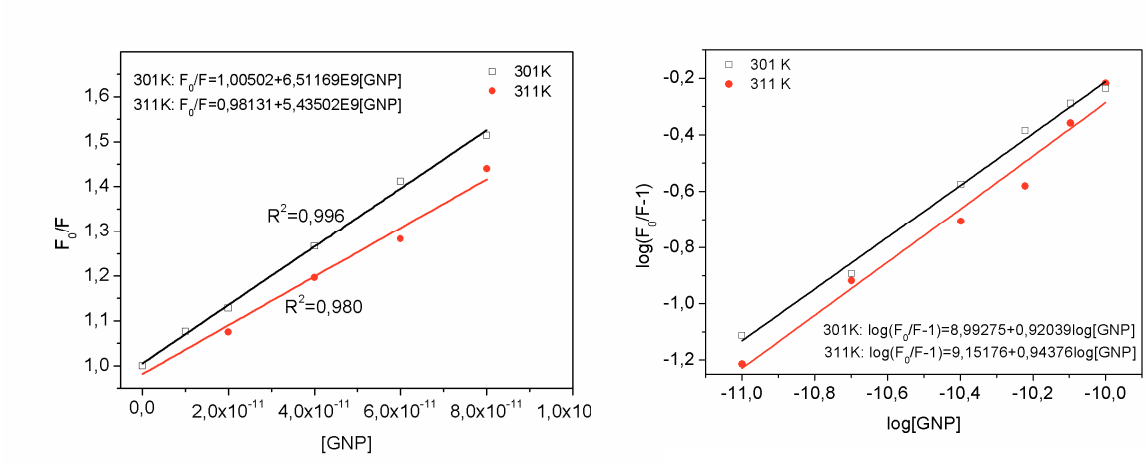

Figure 3-9 (left): Stern-Volmer plot of fluorescence quenching of Hb by GNP at two temperatures. (301K si 311K)

Figure 3-10 (right): Double logarithmic plot of GNP quenching effect on Hb molecules at two temperatures (301 K and 311 K).

Table 3-1: Binding parameters of the interaction between gold nanoparticles and hemoglobin

***T* (K)**	***K*$_{SV}$ (l/mol)**	***K*** **(l/mol)**	***n***
301	6.51×10^{9}	9.8344×10^{8}	0.920
311	5.435×10^{9}	1.4182×10^{9}	0.943

3.4. Electrochemical detection of acrylamide using gold nanoparticles-hemoglobin modified electrodes

3.4.1. Acrylamide and hemoglobin-acrylamide adduct formation

3.4.1.1. Acrylamide: a neurotoxin and potential carcinogen

Acrylamide (*Figure 3-11*) is a neurotoxin and a potential carcinogen, which is found in fried products such as French fries (64–5000 µg/kg were reported in potato-based snacks, baked bread, mainly food products that contain large quantity of starch, processed at high temperatures, but also in coffee, prune juice and cigarette smoking[37].

[37] Parzefall Wolfram - *Food and Chemical Toxicology*, 46 (**2008**), 1360–1364

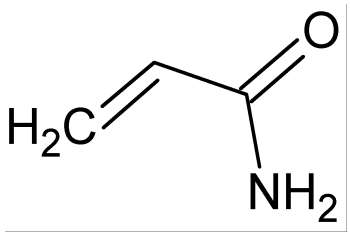

Figure 3-11: Acrylamide structure

The first announcement of presence of acrylamide in processed foods by University of Stockholm and National Food Administration of Sweden was made in 2002[38], and since then efforts were made for the quantitative determination of acrylamide in food products. Chromatographic techniques such as GC–MS with or without bromination, LC and HPLC–MS are mainly used for the determination of acrylamide levels in food products, but they are laborious and expensive. In March 2010, acrylamide was added by the European Chemical Agency in the SVHC list (Substance of Very High Concern[39]), due to its mutagenic and carcinogen effects, and the utilization in the European Union was restricted.

Hemoglobin forms adducts with some classes of molecules, many of them being toxic (acrylamide, acrylonitrile, amino-phenols[40]). By using this property, it is possible to design new detection systems for these classes of molecules.

3.4.1.2. Hemoglobin-acrylamide adduct formation

With acrylamide, hemoglobin forms adducts, due to the interaction between the amino group of N-terminal valine from hemoglobin structure with acrylamide molecule (*Figure 3-12*). Human dietary exposure to acrylamide through hemoglobin adduct determination has been carried out with various analytical methods[41].

[38] http://aa.iacfc.affrc.go.jp/en/
[39] http://en.wikipedia.org/wiki/Substance_of_very_high_concern
[40] von Stedingk H., Rydberg P., Törnqvist M. - *Journal of Chromatography B*, 878 (**2010**), 2483–2490;
[41] Preston A., Terry F., Alistair D., Elliott C.T. - *Journal of Immunological Methods,* 341 (**2009**), 19–29

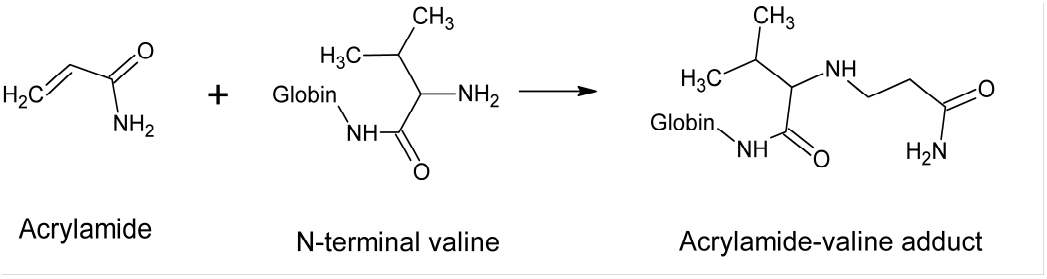

Figure 3-12: Hemoglobin-acrylamide covalent adduct formation

3.4.2. Preparation and characterization of GNP-Hemoglobin modified electrodes

The modified electrodes were obtained by successive deposition of gold nanoparticles and then horse hemoglobin on transparent, conductive ITO glass. Deposition of gold nanoparticles on the silanized glasses was made by inserting the electrodes in GNP solution for 1 h, at 4°C. Then, the electrodes were dipped in hemoglobin solution (1 mg/ml, in PBS) for 12 h, at 4°C. The modified electrodes thus obtained were kept in air until used, without losing their electrochemical properties (in 3 weeks).

The modified electrode was characterized using UV–Vis spectroscopy and AFM microscopy (*Figure 3-14*).

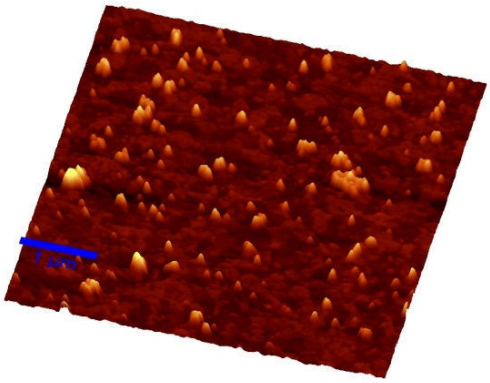

Figure 3-14: AFM image of the modified ITO electrode

The strong absorption band at 545 nm (red line in *Figure 3-15 A*) corresponds to gold nanoparticles attached to ITO substrate. The red shift (21 nm) that appears in the absorption band of nanoparticles attached to the substrate (545 nm) compared to that of nanoparticles in solution (524 nm - *Figure 3-4 A*) arises from the increasing of nanoparticles size due to aggregation, and from the changes that appear in the refraction index of the surrounding medium of nanoparticles. In the case of nanoparticles attached to the substrate, the distance between nanoparticles decreases (creating a more dense packing), compared to that in solution, and there is a strong interaction between the surface of the nanoparticles and the amino group from the silane layer.

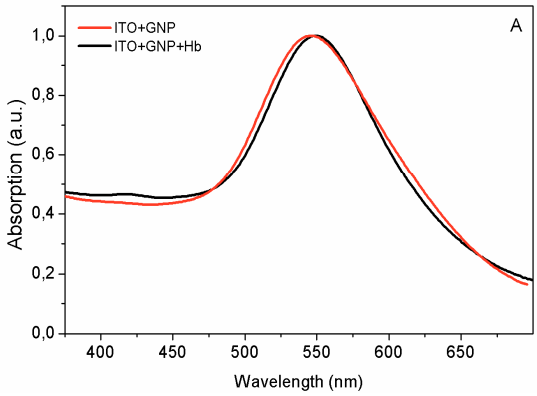

Figure 3-15 A: UV-Vis spectra of the GNP-Hb modified ITO electrode;

Gold nanoparticles act as mediators to enhance the electron transfer process between ITO and hemoglobin and facilitate the binding of hemoglobin onto the electrode.

3.4.3. Acrylamide determination using GNP-Hemoglobin modified electrodes

Being hemoglobin adduct, acrylamide binds to the protein modified electrode, from solution. The electrode is passivated due to that interaction and the redox response of a mediator (ferrocyanide) decreases. Depending on the decreasing percentage, a quantitative determination of acrylamide can be obtained.

Hb–GNP modified ITO glass electrodes were used as working electrodes and a platinum disk was used as counter electrode. The working electrode has an area of 13

mm^2. The electrolyte used for the electrochemical measurements was obtained by adding 5 mM potassium ferrocyanide to 5 ml Phosphate Buffer Saline (PBS) solution. Potassium ferrocyanide was used as redox probe to characterize the modified electrode. Cyclic voltammetry was performed by cycling the potential from -0.2 V to +0.7 V, with scan rate 0.1 V/s. The dependence of the amperometric response on the concentration of the analyte was expressed as currents measured at the peak potentials for the modified electrodes.

Cyclic voltammograms in *Figure 3-20* display the modifications that appear in the current intensity in the presence of low concentrations of acrylamide. These modifications are due to the binding between acrylamide and hemoglobin deposited onto the electrode surface, which decreases the electron transfer rate between the electrolyte and modified electrode.

Due to the formation of hemoglobin–acrylamide adduct the electroactivity of hemoglobin is altered and this results in decreasing the potential peaks in cyclic voltammograms. Differential pulse voltammetry measurements were also performed, but the sensitivity was worse than that obtained by cyclic voltammetry measurements (figures not shown here).

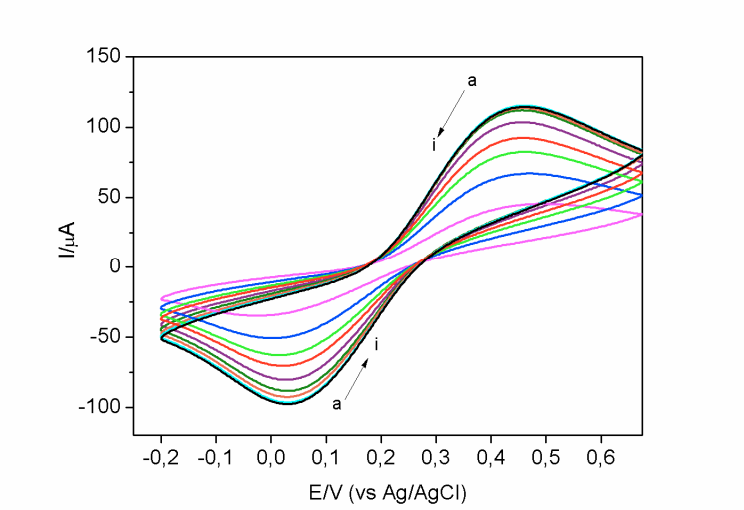

Figure 3-20: Cyclic voltammetry response of Hb–GNP modified ITO electrode toward acrylamide on various concentrations (a-0; b-$4x10^{-8}$; c-$4x10^{-7}$; d-$6x10^{-7}$; e-$18x10^{-7}$; f-$3x10^{-6}$; g-$4x10^{-6}$; h-$6x10^{-6}$; i-10^{-5})

The detection limit is $2x10^{-8}$ M. Taking into consideration a signal-to-noise ratio 3, a concentration as low as 0.1µM can be detected using our electrochemical cell configuration. Measurements were made in the range $10^{-8} \div 10^{-5}$ M, domain where the concentration of the analyte depends linear with the peak intensity (both anodic and cathodic peak-see *Figures 3-21* and *3-22*).

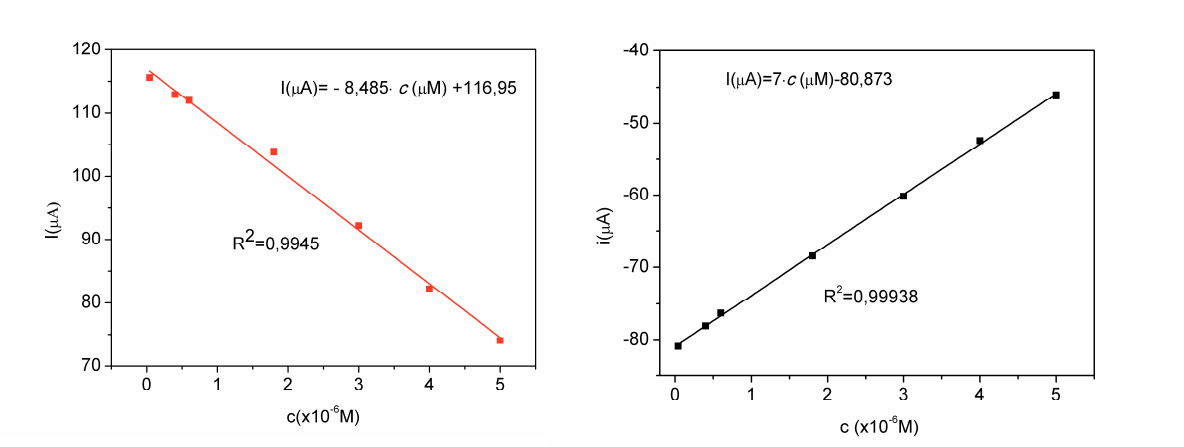

Figure 3-21 (right): Linear dependence of acrylamide concentration on the cathodic peak intensity

Figure 3-22 (left): Linear dependence of acrylamide concentration on the anodic peak intensity

The main disadvantage of this setup is that the binding between hemoglobin and acrylamide implies a strong covalent bond. The bond could be broken using an N-alkyl Edman degradation procedure, but the forces that are implied to attaching gold nanoparticles onto ITO glass, as well as the binding between hemoglobin and gold nanoparticles are weaker. Therefore, our modified electrode can only be used once, because the binding is considered to be irreversible, and ITO electrode has to be modified again prior to a new measurement. However, the procedures for the deposition of the layers onto ITO glass are easy and inexpensive compared with regular detection methods for acrylamide (chromatographic techniques).

As a conclusion: this Hb–GNP–ITO glass electrochemical setup can be successfully used to monitor low concentrations of acrylamide[42] (down to 10^{-8} M).

[42] Garabagiu S., Mihailescu G. - *Journal of Electroanalytical Chemistry*, 659 (**2011**), 196–200

General conclusions and future work

The original aspects of this thesis consist in the fabrication of some nanostructures, the bio-functionalization of gold nanoparticles using a redox protein and the development of a new detection system for a neurotoxin (acrylamide). The main results presented in the thesis are the following:

1. **I fabricated and characterized porous anodic aluminium oxide membranes:**
   - ✓ I Developed a new dissolution method for the barrier layer that exists at the interface between aluminium base and the porous layer;
   - ✓ I studied the optical transmission through the alumina membranes, using both experimental and simulated spectra;
2. **I prepared noble metal nanostructures:**
   - ✓ I electrodeposited metallic nanowires into anodic alumina pores;
   - ✓ Using the dissolution method mentioned above, I prepared a network of silver nanowires, partially embedded into the template, such as every wire is surrounded by the insulating alumina;
3. **I analyzed the bio-functionalization of gold nanoparticles using Hemoglobin molecules:**
   - ✓ I characterized the interaction between gold nanoparticles and hemoglobin using optical spectroscopy;
   - ✓ Fluorescence spectroscopy offers information about the binding constants, stoichiometry and the types of forces involved into the interaction between gold nanoparticles and hemoglobin;
4. **I designed a new electrochemical detection system for acrylamide:**
   - ✓ I fabricated modified ITO electrodes, using gold nanoparticles and hemoglobin;
   - ✓ By obtaining the calibration plots, small concentrations of acrylamide ($10^{-5} \div 10^{-8}$ M) can be detected, by utilizing simple electrochemical methods such as cyclic voltammetry or differential pulse voltammetry;